Solids Modeled by Ab-Initio Crystal Field Methods. Part 17. Study of the Structure and Vibrational Spectrum of Urea in the Gas Phase and in Its $P\bar{4}2_1m$ Crystal Phase

B. Rousseau and C. Van Alsenoy*

Department of Chemistry, University of Antwerp (UIA), Universiteitsplein 1, B-2610 Antwerpen, Belgium

R. Keuleers and H. O. Desseyn

Department of Chemistry, University of Antwerp (RUCA), Groenenborgerlaan 171, B-2020 Antwerpen, Belgium

Received: February 4, 1998; In Final Form: April 27, 1998

In this study the geometrical structure and vibrational spectrum are studied for the urea molecule ($CO(NH_2)_2$) in the gas phase as well as in its $P\bar{4}2_1m$ crystal phase. Experimental frequencies for urea in the crystal phase are determined for the $CO(NH_2)_2$, $C^{18}O(NH_2)_2$, $CO(^{15}NH_2)_2$, $^{13}CO(NH_2)_2$, $CO(ND_2)_2$, $C^{18}O(ND_2)_2$, $CO(^{15}ND_2)_2$, and $^{13}CO(ND_2)_2$ isotopomers. Using calculations at the RHF/6-31++G** level, the equilibrium geometry and harmonic force field for both the gas phase and the crystal phase are determined. The crystal phase is modeled using a 15 molecule cluster surrounded by 5312 point charges. Calculated structure and frequencies are in excellent agreement with experiment. Shifts in frequencies for the above-mentioned isotopomers are reproduced with a root mean square deviation and largest difference of 15 and 43 cm^{-1}, respectively. Shifts in frequencies in going from the gas phase to the crystal phase for the parent and deuterated isotopomer are reproduced with a root mean square deviation and largest difference of 14 and 31 cm^{-1}, respectively.

I. Introduction

Urea has been studied extensively because it is one of the simplest biological molecules and because it is one of the simplest diamides used in organic chemistry. Moreover, it is of interest to inorganic chemistry because of its capability in forming transition metal complexes,[1] and because of its interesting nonlinear optical (NLO) properties, it is applicable in frequency-doubling devices.[2] It is also one of the well-known examples of serendipity in science. In 1828, upon trying to synthesize ammonium cyanides Wöhler[3] obtained urea, thereby rendering untenable the hypothesis of "vitalism" which maintained that organic compounds could only be synthesized through "a vital force" present only in living tissue.

Although a lot of work has been done on urea, there still remains some uncertainty in the interpretation of its vibrational spectrum. In part these problems originated from the fact that the interpretation of its solid-state spectrum was based on gas-phase calculations. For example some authors[4−7] have assigned the band at 1683 cm^{-1} in the solid-state vibrational spectrum of urea to the C−O stretching vibration and the band at 1598 cm^{-1} to the symmetric NH_2 deformation mode, whereas others[8−11] assigned them in reversed order. It will be shown that, on the basis of experimental[12] and calculated data, the latter is the more likely.

A number of quantum chemical calculations on urea in the gas phase, both geometry optimizations and frequency calculations, have appeared in the literature. The earlier calculations[13−17] predicted a planar structure, whereas experimental data[18−21] and more recent calculations[22−26] have shown it to be nonplanar. The problems in the earlier calculations originated either in the use of inadequate methods or the use of too small basis sets. As far as we know, the only calculations on crystalline urea are the single point energy calculations performed using the periodic Hartree−Fock[27] method by Dovesi et al.,[28] Gatti et al.,[29] and Starikov[30] in which mainly the electronic band structure and charge distribution were studied which are not directly relevant to this work.

This work aims at giving a definite assignment of the bands in the vibrational spectrum of urea, both in the solid state and in the gas phase. To achieve this, the structure and vibrational spectrum of urea were calculated for a free molecule as well as crystalline urea and compared with the corresponding experimental spectra recorded for eight isotopomers. The full experimental vibrational analysis based on the infrared and Raman spectra of these isotopomers at room temperature and at −196 °C as well as at elevated pressure and in solution will be discussed in a forthcoming paper.[12] This study compares the calculated and experimental frequencies. Moreover, it will be shown that the molecular cluster approach describing the crystalline state allows one to predict isotopic as well as gas-to-crystal phase shifts in frequencies to high accuracy. It proves that this allows an accurate description of molecular crystals even in the case of extensively hydrogen bonded systems, such as urea.

II. Theoretical Model and Computational Procedure

Molecular crystals can be studied either by use of the periodic Hartree−Fock method[27] or by molecular cluster methods.[31,32] The former has the advantage that the periodicity of the system is included directly into the wave function. The latter, however, has the advantage of its conceptual simplicity and the fact that existing quantum mechanical codes can be used in which analytical gradients, essential for geometry optimizations, are available. Numerous successful calculations[31,33,34] have shown that the cluster method allows efficient and accurate studies of molecular crystals.

* To whom correspondence should be addressed.

S1089-5639(98)01008-1 CCC: $15.00
Published on Web 07/17/1998

In the molecular cluster methods two models are frequently used: the point charge model (PC model)[31,33] and the supermolecule model (SM model).[34] In the PC model a molecule described by a wave function is surrounded in accordance with the symmetry of the crystal, by point charges. In the SM model a cluster is constructed from a molecule and its nearest neighbors, described by a wave function and surrounded by point charges.

The combination of the SM model with conventional Hartree−Fock methods requires prohibitively expensive calculations, even for medium sized molecules. To allow calculations on large systems, the MIA approach,[35,36] an efficient combination of the direct SCF method[37] and the multiplicative integral approximation (MIA approximation),[35] was developed and implemented in the quantum chemical program package BRABO.[36]

In the MIA approximation a product of two Gaussians, one with a high exponent (χ_μ) and one with a low exponent (χ_ν), is expanded in a set of auxiliary functions ($\chi_{\mu,\alpha}$) derived from χ_μ:

$$\chi_\mu\chi_\nu = \sum_\alpha c_\alpha \chi_{\mu,\alpha} \tag{1}$$

Because the auxiliary functions only depend on χ_μ, this expansion reduces a four-function two-electron integral to a linear combination of three-function two-electron integrals:

$$(\mu\nu|\lambda\sigma) = \sum_\alpha c_\alpha^{\mu\nu}(\mu_\alpha|\lambda\sigma) \tag{2}$$

The fact that the two-electron integral $(\mu_\alpha|\lambda\sigma)$ is independent of the index ν allows a rapid buildup of the Fock matrix. The resulting Fock matrix is not exact because the expansion (1) is not exact. However, those two-electron integrals for which the error, estimated using (3), is larger than a preset threshold are

$$\Delta_{\mu\nu\lambda\sigma} = \frac{\Delta Q_{\mu\nu} S_{\lambda\sigma}}{r_{\mu,\lambda\sigma}^3} \Delta P_{\mu\nu\lambda\sigma} \tag{3}$$

systematically corrected, thereby yielding wave functions and energies identical to those obtained using the conventional method. A detailed explanation of the quantities used in (3) can be found in the literature.[35,36] Combining the MIA approximation with the direct-SCF approach makes the number of two-electron integrals that needs correction to decrease rapidly as the calculation converges. Thus, combination of the MIA approximation and the direct SCF method yields an efficient method, scaling linearly with the size of the system,[38] for SCF calculations on large systems such as the 46-peptide crambin.[39]

In this study the $P\bar{4}2_1m$ crystal phase[40] of urea was modeled using the SM approach in which the supermolecule was constructed from a central molecule surrounded by its 14 nearest neighbors generated using the symmetry operations given in Table 1. A projection of the cluster is shown in Figure 1. This supermolecule was surrounded by molecules, represented by Mulliken point charges,[41] having an atom nearer than 20 Å to any central-molecule atom, yielding 664 neighboring molecules (5312 point charges). Use of the same basis set to describe the gas phase and crystal phase is desirable in order not to hamper comparisons with basis set effects, while use of polarization and diffuse functions is necessary to obtain, in accordance with experiment, a nonplanar equilibrium gas-phase geometry. Therefore a 6-31++G** basis set was chosen for this study. Use of this basisset results in a total of 100 basis functions describing a single molecule and 1500 basis functions describing the supermolecule cluster.

TABLE 1: Space Group, Cell Parameters,[a] and Symmetry Operations Used to Generate the 14 Nearest Neighbors Surrounding a Urea Molecule

space group	$P\bar{4}2_1$m		
cell parameters	$a = b = 5.565$ Å $c = 4.684$ Å		
neighbor	symmetry operation[b]		
1	$-1 + x$	y	z
2	$-1/2 + x$	$-x$	$-z$
3	$-1/2 + x$	$-x$	$1 - z$
4	$-1/2 + x$	$1 - x$	$-z$
5	$-1/2 + x$	$1 - x$	$1 - z$
6	x	$-1 + y$	z
7	x	y	$-1 + z$
8	$1/2 + x$	$-x$	$-z$
9	x	y	$1 + z$
10	$1/2 + x$	$-x$	$1 - z$
11	x	$1 + y$	z
12	$1/2 + x$	$1 - x$	$-z$
13	$1/2 + x$	$1 - x$	$1 - z$
14	$1 + x$	y	z

[a] Neutron diffraction study at 12 K.[40] [b] Symmetry operations are given under the assumption that coordinates of the atoms of the central molecule are represented by (x,y,z).

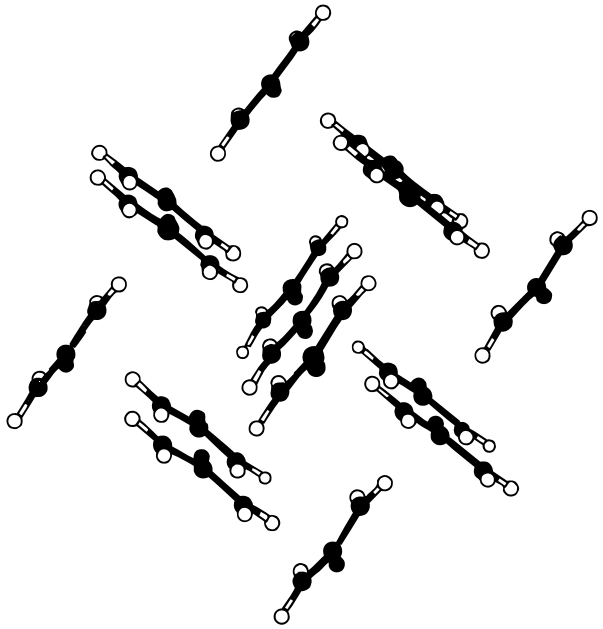

Figure 1. Projection of the 15 molecule cluster used to model the $P42_1m$ crystal phase of urea.

A full geometry optimization was performed on urea in both the gas phase and the solid state using standard gradient techniques[42] (fixing the unit cell parameters as well as the space group symmetry to their respective experimental values[40]). For a detailed description of the procedure used to optimize the structure of these clusters we refer to the literature.[33,34] Optimized geometries were subsequently used in a numerical force field calculation for which analytic gradients were calculated at geometries described by displacements along the symmetry coordinates given in Table 2. Atom numbering is given in Figure 2. Frequencies for all isotopomers were calculated by solving the Wilson equation.[43]

III. Experimental Section

The normal urea used was a pure commercial product, available at Aldrich (U270-9) just as $CO(ND_2)_2$ (17,608-7),

TABLE 2: Symmetry Coordinates of Urea (for Atom Numbers see Figure 2; Symmetry Assignments Are Those Based on a Planar C_{2v} Geometry)

	specification[a]	assignment	symmetry
1	$r(C_1-O_2)$	ν(CO)	A_1
2	$r(C_1-N_3)+r(C_1-N_6)$	ν_s(CN)	A_1
3	$r(N_3-H_4)+r(N_3-H_5)+r(N_6-H_7)+r(N_6-H_8)$	$\nu_s(NH_2)$	A_1
4	$r(N_3-H_4)-r(N_3-H_5)+r(N_6-H_7)-r(N_6-H_8)$	$\nu_a(NH_2)$	A_1
5	$2\theta(N_3-C_1-N_6)-\theta(O_2-C_1-N_3)-\theta(O_2-C_1-N_6)$	δ(CN)	A_1
6	$2\theta(H_4-N_3-H_5)-\theta(C_1-N_3-H_4)-\theta(C_1-N_3-H_5)+2\theta(H_7-N_6-H_8)-\theta(C_1-N_6-H_7)-\theta(C_1-N_6-H_8)$	$\delta_s(NH_2)$	A_1
7	$\theta(C_1-N_3-H_4)-\theta(C_1-N_3-H_5)+\theta(C_1-N_6-H_7)-\theta(C_1-N_6-H_8)$	$\rho_s(NH_2)$	A_1
8	$\tau(O_2-C_1-N_3-H_4)+\tau(N_6-C_1-N_3-H_4)+\tau(O_2-C_1-N_3-H_5)+\tau(N_6-C_1-N_3-H_5)+\tau(O_2-C_1-N_6-H_7)+\tau(N_3-C_1-N_6-H_7)+\tau(O_2-C_1-N_6-H_8)+\tau(N_3-C_1-N_6-H_8)$	$\tau_s(NH_2)$	A_2
9	$\chi(N_3,C_1,H_4,H_5)+\chi(N_6,C_1,H_7,H_8)$	$\omega_s(NH_2)$	A_2
10	$\tau(O_2-C_1-N_3-H_4)+\tau(N_6-C_1-N_3-H_4)+\tau(O_2-C_1-N_3-H_5)+\tau(N_6-C_1-N_3-H_5)-\tau(O_2-C_1-N_6-H_7)-\tau(N_3-C_1-N_6-H_7)-\tau(O_2-C_1-N_6-H_8)-\tau(N_3-C_1-N_6-H_8)$	$\tau_a(NH_2)$	B_1
11	$\chi(C_1,O_2,N_3,N_6)$	ω(CO)	B_1
12	$\chi(N_3,C_1,H_4,H_5)-\chi(N_6,C_1,H_7,H_8)$	$\omega_a(NH_2)$	B_1
13	$r(C_1-N_3)-r(C_1-N_6)$	ν_a(CN)	B_2
14	$r(N_3-H_4)+r(N_3-H_5)-r(N_6-H_7)-r(N_6-H_8)$	$\nu_s(NH_2)$	B_2
15	$r(N_3-H_4)-r(N_3-H_5)-r(N_6-H_7)+r(N_6-H_8)$	$\nu_a(NH_2)$	B_2
16	$\theta(O_2-C_1-N_3)-\theta(O_2-C_1-N_6)$	δ(CO)	B_2
17	$2\theta(H_4-N_3-H_5)-\theta(C_1-N_3-H_4)-\theta(C_1-N_3-H_5)-2\theta(H_7-N_6-H_8)+\theta(C_1-N_6-H_7)+\theta(C_1-N_6-H_8)$	$\delta_a(NH_2)$	B_2
18	$\theta(C_1-N_3-H_4)-\theta(C_1-N_3-H_5)-\theta(C_1-N_6-H_7)+\theta(C_1-N_6-H_8)$	$\rho_a(NH_2)$	B_2

[a] r(i−j), bond length between atoms i and j; θ(i−j−k), valence angle between atoms i, j, and k; τ(i−j−k−l), torsion angle between atoms i, j, k, and l; χ(i,j,k,l), out-of-plane deformation of atom i out of the j, k, l plane.

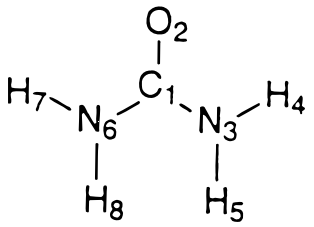

Figure 2. Atom numbering for the urea molecule.

$^{13}CO(NH_2)_2$ (29,935-9), and $CO(^{15}NH_2)_2$ (31,683-0). $C^{18}O(NH_2)_2$ was synthesized according to the method used by Korn[44] and Laulicht et al.[9] by dissolving 100 mg of pure cyanamide in a mixture of 1 mL of $H_2{}^{18}O$ and 0.2 mL of concentrated hydrochloric acid. After this, the solution was refluxed for 10 min. It was cooled, neutralized with sodium carbonate, and evaporated to dryness in vacuo. The residue was pure enough and did not need any further purification. Deuterated $^{13}CO(NH_2)_2$, $CO(^{15}NH_2)_2$, and $C^{18}O(NH_2)_2$ were prepared by dissolving the products in D_2O and evaporating the solution to dryness in vacuo. This procedure was repeated three times.

The low-temperature (−196 °C) infrared spectra were recorded on a Bruker IFS 113v Fourier transform spectrometer, using a liquid nitrogen cooled MCT detector with a resolution of 1 cm^{-1}. For each spectrum 200 scans were recorded and averaged. These measurements were performed with a laboratory designed liquid nitrogen cooled cryostat,[45] consisting of a copper sample holder with a small container which can be filled with liquid nitrogen. This is surrounded by a jacket with KBr windows and placed under vacuum. From the sample a pellet with KBr as a matrix was made.

IV. Geometry

In Table 3 experimental and calculated geometries are compared. A nonplanar experimental gas-phase geometry was obtained in accordance with earlier data[18−20] and a study by Godfrey et al.[21] using microwave spectroscopy. The experimental solid-state geometry was taken form a neutron diffraction study at 12 K by Swaminathan et al.[40] In the crystal the molecules are lined up to form infinite ribbons, and urea has, contrary to the gas phase, a planar geometry.[40,46−49] Neighboring ribbons are orthogonal to each other, and the molecules in neighboring ribbons are positioned in opposite directions. Every oxygen atom participates in four hydrogen bonds, two within the tape and two between adjoining ribbons. The structure of the urea crystal is depicted in Figure 1.

As can be seen from Table 3, agreement is as good as can be expected in view of the level of the theory used. For the solid-state structure, differences amount to a maximum 0.02 Å for bond lengths and 0.6° for valence angles. Except for CO and CN bond lengths, differences between theory and experiment are within 3σ. Differences between theory and experiment are somewhat larger for the gas-phase structure, in particular with respect to the N−H_4 bond distance and the H_4NH_5 valence angle. We would, however, like to point out that the microwave r_s geometry, obtained by solving the Kraitchman[50] equations, is known[51] to have large error bars on coordinates of atoms close to an inertial plane. This is particularly the case for the *b*-coordinate of H_4. This large uncertainty may be the cause of the unusually large discrepancy between theory and experiment for the N−H_4 bond length. In Table 4 experimental rotational constants are compared with those calculated using the experimental r_s geometry and our optimized gas-phase structure given in Table 3. As can be seen, our calculated structure (Δ_1) has a much larger systematic error in comparison with the rotational constants calculated using the experimental structure (Δ_{exp}). If, however, in our theoretical structure the CO bond length is increased by 0.02 Å and the CN bond length by 0.01 Å, in accordance with the solid-state differences, agreement between calculated and experimental rotational constants surpasses that of the experimental structure. This leads to the conclusion that the differences found between theory and experiment for the gas-phase structure may be attributed to deficiencies in the procedure used to extract structural information from the experimental data.

Comparing calculated and experimental shifts in geometrical parameters in going from the gas phase to the crystal phase (Table 3, columns Δ_{exp} and Δ_{calc}), the C−O bond length is found to increase by 0.04 Å while the C−N bond is found to decrease by almost the same amount. The magnitude of these shifts is in excellent agreement with shifts predicted in the literature.[52] On the basis of a study of the structure of a N−C═O unit in crystals

TABLE 3: Comparison between Calculated and Experimental Structural Parameters for the Gas Phase and the Crystal Phase of Urea

	gas phase			crystal phase			Δ^a	
	r_e[b]	r_s[c]	δ	r_e[d]	r_α[e]	δ	calc	exp
				Bond Lengths[f]				
CO	1.200	1.221	−0.021	1.242	1.265(1)	−0.023	0.042	0.044
CN	1.370	1.378	−0.008	1.331	1.349(1)	−0.018	−0.039	−0.029
NH_4	0.999	1.021	−0.022	0.999	1.008(4)	−0.009	0.000	0.013
NH_5	0.998	0.998	0.000	0.999	1.001(4)	−0.002	0.001	0.003
				Valence Angles[f]				
OCN	122.7	122.6	0.1	121.2	121.4(1)	−0.2	−1.5	−1.2
NCN	114.6	114.7	−0.1	117.6	117.2(1)	0.4	3.0	2.5
CNH_4	114.1	112.8	1.3	119.3	119.1(1)	0.2	5.2	6.3
CNH_5	118.7	119.2	−0.5	120.9	120.5(1)	0.4	2.2	1.3
H_4 NH_5	115.3	118.6	−3.3	119.8	120.4(2)	−0.6	4.5	1.8
				Torsion Angles[f]				
$OCNH_4$	−12.5	−10.8	−1.7	0	0	0	12.5	10.8
$OCNH_5$	−153.7	−156.9	3.2	−180	−180	0	−26.3	−23.1
$NCNH_4$	167.5	169.2	−1.7	180	180	0	12.5	10.8

[a] Experimental (Δ_{exp}) and calculated (Δ_{calc}) differences between gas-phase and crystal-phase structures. [b] RHF/6-31++G** calculation. [c] Microwave study.[21] [d] RHF/6-31++G** calculation using SM model. [e] Neutron diffraction study at12 K.[40] Values corrected for harmonic motion and anharmonic bond stretching. [f] Bond lengths in Ångströms; valence and torsion angles in degrees.

TABLE 4: Experimental Rotational Constants (exp, MHz) and Differences between Experimental and Calculated Values Obtained Using the Experimental r_s Structure (Δ_{exp}), the Calculated r_e Structure (Δ_1), and the Corrected r_e Structure (Δ_2)[a]

	exp[21]	Δ_{exp}	Δ_1	Δ_2
		$(NH_2)CO(NH_2)$		
A	11 233	20	285	12
B	10 369	28	142	2
C	5 417	16	118	16
		$(NH_2)CO(NHD)$		
A	11 225	24	287	14
B	9 590	23	130	3
C	5 197	15	111	15
		$(NH_2)CO(NDH)$		
A	10 826	28	253	17
B	9 895	21	150	−1
C	5 204	14	112	16
		$(^{15}NH_2)CO(^{15}NH_2)$		
A	11 027	19	279	11
B	9 828	25	134	0
C	5 220	15	112	14
		$(NH_2)C^{18}O(NH_2)$		
A	10 466	17	264	8
B	10 369	28	142	2
C	5 231	16	115	15

[a] $r_e(CO) + 0.02$ Å; $r_e(CN) + 0.01$ Å.

using the Cambridge Crystallographic Data Base,[53] these authors found a lengthening of the CO bond and concurrent shortening of the CN bond with respectively 0.011 and 0.015 Å per hydrogen bond formed, explaining the shift of 0.04 Å, the carbonyl oxygen taking part in four hydrogen bonds. For valence and torsion angles, differences in shifts between calculated and experimental values can again be attributed to uncertainties in the experimental geometry.

V. Vibrational Spectrum

Since it is well-known[54] that Hartree−Fock calculations overestimate the force constants by about 10−20%, the calculated force constants are scaled using the relation

$$k'_{ij} = [\alpha_i \alpha_j]^{1/2} k_{ij}$$

TABLE 5: Definition of Groups of Symmetry Coordinates[a] Used in the Scaling of the Calculated Force Field with Optimized Scale Factors

crystal phase		gas phase	
$\nu(NH_2)$ (q_3, q_4, q_{14}, q_{15})	0.79	$\nu(CO)$ (q_1)	0.77
other	0.81	other	0.82

[a] See Table 2 for a definition of the symmetry coordinates.

Using a least-squares procedure, two scale factors were optimized separately for the gas phase and the crystal phase by fitting experimental and calculated frequencies for the parent isotopomer of urea. Optimized values for these scale factors are given in Table 5. Scaled force constants are given in Table 6. For the gas-phase experimental values were taken from King[18] (Table 7). Experimental values for the crystal phase were determined in this study (Table 8).[12] Calculated and experimental frequencies are compared for the gas phase and the crystal phase respectively in Table 7 and Table 8. For the gas phase, treating the CO-stretch coordinate separate from the other coordinates, the scaling resulted in a fit between experimental and calculated frequencies with a root mean square deviation and maximum difference of 11 and 26 cm^{-1}, respectively. For the crystal phase, treating the $\nu_s(NH_2)$ and $\nu_a(NH_2)$ coordinates separate from the others, it resulted in an optimal fit with a root mean square deviation and maximum difference of 9 and 25 cm^{-1}, respectively. Use of a single scale factor of 0.8, the recommended value for Hartree−Fock force constants,[54] yields much larger deviations between theory and experiment. For example, for the parent isotopomer, root mean square and largest deviation deteriorate respectively to 27 and 52 cm^{-1} in the gas phase and to 17 and 39 cm^{-1} in the crystal phase. In view of this marked deterioration of the results, more than a factor of 2, use of different scale factors is justifiable.

A. Gas-Phase Spectrum. To our knowledge, up till now only two matrix isolation spectra[18,20] and one gas-phase spectrum[55] have appeared in the literature of urea. Li et al.[20] did not give any assignments while the assignments of Langer et al.[55] are rather doubtful in view of the existing literature and the data presented in this work (details will be given below). The overall (parent and deuterated isotopomer) root mean square deviation and the maximum difference, being 14 and 28 cm^{-1}, respectively, are only slightly different from the corresponding values for the parent molecule which was used for the determination

TABLE 6: Scaled Force Constants (×100, in mdyne Å^{-1} and mdyne rad^{-1}, for the Symmetry Coordinates of Table 2) for the Gas-Phase and Crystal-Phase (SM Model) Structure

S[a]	C[b]	force constants								
		Gas Phase								
A	1	1135								
	2	153	676							
	3	−4	−3	673						
	4	−2	2	0	678					
	5	−50	40	−1	11	115				
	6	−7	−11	9	−3	−6	51			
	7	−6	2	3	12	18	1	59		
	8	−1	1	0	1	4	−1	0	3	
	9	3	−21	−12	1	0	−2	−3	−1	8
B	10	5								
	11	0	72							
	12	−2	3	8						
	13	−4	3	−24	556					
	14	−1	4	−11	1	672				
	15	1	−1	0	3	1	677			
	16	−1	−2	−1	49	−1	−7	114		
	17	1	−4	−2	−3	8	−3	−1	50	
	18	2	−1	−2	−1	2	11	−14	1	55
		Crystal Phase								
A_1	1	957								
	2	154	836							
	3	−15	0	640						
	4	−3	−2	−3	641					
	5	−63	46	1	6	131				
	6	−7	−25	3	2	−4	48			
	7	−6	−3	−4	5	3	1	63		
A_2	8	8								
	9	1	5							
B_1	10	11								
	11	0	76							
	12	−1	9	7						
B_2	13	662								
	14	18	634							
	15	0	−1	639						
	16	55	−7	−4	119					
	17	−16	2	3	−4	46				
	18	1	−4	6	−9	0	56			

[a] Symmetry. [b] Coordinate.

of the optimal scale factors, indicating an optimal agreement for both isotopomers. The calculated frequencies and assignments are in excellent agreement with the spectrum of King[18] as reassigned by Vijay et al.[17] and Spoliti et al.[56] Langer et al.[55] assigned the $\delta_a(NH_2)$, $\rho_a(NH_2)$, and the $\nu_s(CN)$ modes to bands at 1749, 1157, and 1032 cm^{-1}, respectively. Vijay et al.[17] and Spoliti et al.[56] assigned these modes, on the basis of the experimental frequencies obtained by King, to bands at 1594, 1014, and 960 cm^{-1}, respectively. Our calculated frequencies for these modes, 1600, 1027, and 934 cm^{-1}, respectively, are in disagreement with the results from Langer et al.[55] but in agreement with the frequencies observed by King[18] as reassigned by Vijay et al.[17] and Spoliti et al.[56]

The assignments as given in Table 7 are in good agreement with those obtained from a B3-LYP/6-311++G(2d,p) calculation by Spoliti et al.[56] who used a single scale factor of 0.98. Deviations from experiment in Spoliti's study are largest for the $\nu(NH_2)$ modes. Errors range between 120 and 130 cm^{-1} and 65−75 cm^{-1} for the parent and deuterated isotopomer, respectively. Moreover, the $\tau_a(NH_2)$ and $\omega_a(NH_2)$ modes were assigned in reversed order. The root mean square deviation between their calculated frequencies and the experimental frequencies is 65 cm^{-1}, and the largest deviation is 128 cm^{-1}.

B. Crystal Phase Spectrum. Using the experimental techniques described above, solid-state infrared spectra were recorded for the crystal phase of the following isotopomers of

TABLE 7: Gas-Phase Experimental[a,b] (ν_{exp}) and Calculated (ν_{calc}) Frequencies (cm^{-1}) and Potential Energy Distribution (PED) for the Parent and Deuterated Isotopomer of Urea

assignment	ν_{calc}	ν_{exp}	δ^c	S[d]	PED[e]
			$CO(NH_2)_2$		
$\nu_a(NH_2)$	3542	3548	−6	A	4(100)
$\nu_a(NH_2)$	3541	3548	−7	B	15(100)
$\nu_s(NH_2)$	3435	3440	−5	A	3(100)
$\nu_s(NH_2)$	3431	3440	−9	B	14(100)
$\nu(CO)$	1731	1734	−3	A	1(64) − 2(15)
$\delta_a(NH_2)$	1600	1594	6	B	17(84) + 13(13)
$\delta_s(NH_2)$	1589	1594	−5	A	6(88)
$\nu_a(CN)$	1386	1394	−8	B	13(54) − 16(21) + 18(14) − 17(11)
$\rho_s(NH_2)$	1149			A	7(76) − 1(19)
$\rho_a(NH_2)$	1027	1014	13	B	18(73) − 13(24)
$\nu_s(CN)$	934	960	−26	A	2(90)
$\omega(CO)$	785	790	−5	B	11(86)
$\delta(CO)$	567	578	−11	B	16(79) + 18(12)
$\omega_s(NH_2)$	518			A	9(78)
$\tau_a(NH_2)$	516			B	10(42) − 12(36)
$\delta(CN)$	466			A	5(78) − 7(20)
$\omega_a(NH_2)$	422	410	12	B	12(50) + 10(38) + 13(10)
$\tau_s(NH_2)$	347			A	8(63) + 9(24)
			$CO(ND_2)_2$		
$\nu_a(ND_2)$	2623	2648	−25	A	4(99)
$\nu_a(ND_2)$	2620	2648	−28	B	15(99)
$\nu_s(ND_2)$	2485	2505	−20	A	3(98)
$\nu_s(ND_2)$	2480	2505	−25	B	14(99)
$\nu(CO)$	1707	1723	−16	A	1(73) − 2(14)
$\nu_a(CN)$	1407	1408	−1	B	13(68) − 16(17) + 17(11)
$\delta_s(ND_2)$	1219	1223	−4	A	6(79) + 2(17)
$\delta_a(ND_2)$	1135			B	17(83)
$\rho_s(ND_2)$	968			A	7(51) + 5(14) − 1(14) − 2(13)
$\rho_a(ND_2)$	839			B	18(49) − 11(35)
$\nu_s(CN)$	830	845	−15	A	2(66) + 7(20) − 6(13)
$\omega(CO)$	756			B	11(62) + 18(16) − 13(12)
$\delta(CO)$	512	517	−5	B	16(67) + 18(29)
$\omega_s(ND_2)$	410			A	9(63) + 5(20)
$\delta(CN)$	390			A	5(51) − 7(26) − 9(18)
$\omega_a(ND_2)$	377			B	12(53) − 10(36)
$\tau_a(ND_2)$	322			B	10(45) + 12(45)
$\tau_s(ND_2)$	247			A	8(67) + 9(23)

[a] Infrared frequencies from King.[18] [b] Parent molecule frequencies used in the least-squares determination of the optimal scale factors. [c] $\nu_{calc} - \nu_{exp}$. [d] Symmetry. [e] Potential energy distribution. See Table 2 for the definition of the symmetry coordinates. The procentual contribution of each coordinate is given between parentheses. Only contributions larger than 10% are listed.

urea: $CO(NH_2)_2$, $C^{18}O(NH_2)_2$, $CO(^{15}NH_2)_2$, $^{13}CO(NH_2)_2$, $CO(ND_2)_2$, $C^{18}O(ND_2)_2$, $CO(^{15}ND_2)_2$, and $^{13}CO(ND_2)_2$. The overall root mean square deviation and largest difference for the eight isotopomers investigated are 13 and 33 cm^{-1}, respectively. Deviations are largest for the deuterated species, probably due to partial deuteration. If these species (four isotopomers) are omitted from the comparison, the root mean square deviation and largest difference reduce to 10 and 29 cm^{-1}, respectively, in close agreement with the corresponding values for the gas-phase frequencies. Taking the level of theory used for the calculation into account, agreement between theory and experiment can again be termed as excellent. The full experimental vibrational analysis will be given elsewhere.[12]

$\nu(NH_2)$ Modes. In the 3300−3500 cm^{-1} region of the spectrum of the parent compound, two double bands are observed. These bands can be attributed to the four NH_2 stretching modes. The band with the highest frequency contains predominately the antisymmetric modes, whereas the other contains the symmetric modes, in agreement with expectations. Within each band the A_1 mode is found at a higher frequency than the B_2 mode. Most authors[4,5,7,9,10,57] observed only two bands instead of four, except Duncan et al.[11] and Vijay et al.[17]

TABLE 8: Crystal-Phase Experimental[a,b] (ν_{exp}) and Calculated (ν_{calc}) Frequencies (cm^{-1}) and Potential Energy Distribution (PED) for a Number of Isotopomers of Urea

assignment	ν_{calc}	ν_{exp}	δ^c	S[d]	PED[e]	assignment	ν_{calc}	ν_{exp}	δ^c	S[d]	PED[e]
					$CO(NH_2)_2$						
$\nu_a(NH_2)$	3460	3448	12	A_1	4(99)	$\rho_a(NH_2)$	1062	1055	7	B_2	18(81) − 13(19)
$\nu_a(NH_2)$	3452	3435	17	B_2	15(100)	$\nu_s(CN)$	1013	1008	5	A_1	2(84)
$\nu_s(NH_2)$	3347	3345	2	A_1	3(99)	$\omega(CO)$	797	790	7	B_1	11(89) + 10(10)
$\nu_s(NH_2)$	3326	3330	−4	B_2	14(100)	$\tau_a(NH_2)$	730	727	3	B_1	10(87) − 11(12)
$\delta_s(NH_2)$	1658	1683	−25	A_1	6(51) − 1(21) + 2(19)	$\tau_s(NH_2)$	602			A_2	8(100)
$\delta_a(NH_2)$	1631	1627	4	B_2	17(72) + 13(24)	$\delta(CO)$	576	568	8	B_2	16(86) + 18(11)
$\nu(CO)$	1597	1598	−1	A_1	1(41) + 6(33) + 7(10)	$\delta(CN)$	540	532	8	A_1	5(89) − 7(10)
$\nu_a(CN)$	1469	1471	−2	B_2	13(54) − 17(21) − 16(15)	$\omega_a(NH_2)$	512	508	4	B_1	12(92)
$\rho_s(NH_2)$	1153	1149	4	A_1	7(70) − 1(28)	$\omega_s(NH_2)$	463			A_2	9(97)
					$C^{18}O(NH_2)_2$						
$\nu_a(NH_2)$	3460	3447	13	A_1	4(99)	$\rho_a(NH_2)$	1062	1055	7	B_2	18(81) − 13(18)
$\nu_a(NH_2)$	3452	3434	18	B_2	15(100)	$\nu_s(CN)$	1002	1005	−3	A_1	2(83) + 1(12)
$\nu_s(NH_2)$	3347	3343	4	A_1	3(99)	$\omega(CO)$	793	784	9	B_1	11(90)
$\nu_s(NH_2)$	3326	3328	−2	B_2	14(100)	$\tau_a(NH_2)$	729	722	7	B_1	10(89) − 11(11)
$\delta_s(NH_2)$	1653	1676	−23	A_1	6(62) + 2(17) − 1(15)	$\tau_s(NH_2)$	602			A_2	8(100)
$\delta_a(NH_2)$	1631	1626	5	B_2	17(72) + 13(24)	$\delta(CO)$	563	561	2	B_2	16(86) + 18(10)
$\nu(CO)$	1586	1589	−3	A_1	1(44) + 6(23) + 7(13) + 5(11)	$\delta(CN)$	535	528	7	A_1	5(89) − 7(10)
$\nu_a(CN)$	1468	1470	−2	B_2	13(54) − 17(21) − 16(15)	$\omega_a(NH_2)$	512	505	7	B_1	12(92)
$\rho_s(NH_2)$	1138	1136	2	A_1	7(70) − 1(28)	$\omega_s(NH_2)$	464			A_2	9(97)
					$CO(^{15}NH_2)_2$						
$\nu_a(NH_2)$	3448	3437	11	A_1	4(99)	$\rho_a(NH_2)$	1053	1046	7	B_2	18(81) − 13(19)
$\nu_a(NH_2)$	3441	3422	19	B_2	15(100)	$\nu_s(CN)$	992	987	5	A_1	2(85)
$\nu_s(NH_2)$	3342	3334	8	A_1	3(99)	$\omega(CO)$	796	788	8	B_1	11(88) + 10(12)
$\nu_s(NH_2)$	3322	3317	5	B_2	14(100)	$\tau_a(NH_2)$	728	725	3	B_1	10(86) − 11(14)
$\delta_s(NH_2)$	1650	1676	−26	A_1	6(50) − 1(23) + 2(18)	$\tau_s(NH_2)$	602			A_2	8(100)
$\delta_a(NH_2)$	1619	1615	4	B_2	17(75) + 13(21)	$\delta(CO)$	570	562	8	B_2	16(86) + 18(10)
$\nu(CO)$	1596	1598	−2	A_1	1(41) + 6(34)	$\delta(CN)$	533	531	2	A_1	5(90)
$\nu_a(CN)$	1464	1466	−2	B_2	13(56) − 17(18) − 16(16)	$\omega_a(NH_2)$	509	500	9	B_1	12(91)
$\rho_s(NH_2)$	1146	1142	4	A_1	7(71) − 1(27)	$\omega_s(NH_2)$	460			A_2	9(97)
					$^{13}CO(NH_2)_2$						
$\nu_a(NH_2)$	3460	3454	6	A_1	4(99)	$\rho_a(NH_2)$	1061	1056	5	B_2	18(80) − 13(20)
$\nu_a(NH_2)$	3452	3433	19	B_2	15(100)	$\nu_s(CN)$	1013	1010	3	A_1	2(85)
$\nu_s(NH_2)$	3347	3337	10	A_1	3(99)	$\omega(CO)$	776	763	13	B_1	11(79) + 10(21)
$\nu_s(NH_2)$	3326	3316	10	B_2	14(100)	$\tau_a(NH_2)$	726	727	−1	B_1	10(76) − 11(24)
$\delta_s(NH_2)$	1647	1676	−29	A_1	6(76) + 2(13)	$\tau_s(NH_2)$	602			A_2	8(100)
$\delta_a(NH_2)$	1624	1624	0	B_2	17(79) + 13(19)	$\delta(CO)$	574	563	11	B_2	16(86) + 18(11)
$\nu(CO)$	1566	1568	−2	A_1	1(52) + 7(13) + 6(12) − 2(12) + 5(11)	$\delta(CN)$	538	531	7	A_1	5(89) − 7(10)
$\nu_a(CN)$	1436	1444	−8	B_2	13(59) − 16(16) − 17(15) + 18(11)	$\omega_a(NH_2)$	512	510	2	B_1	12(92)
$\rho_s(NH_2)$	1153	1144	9	A_1	7(69) − 1(29)	$\omega_s(NH_2)$	463			A_2	9(97)
					$CO(ND_2)_2$						
$\nu_a(ND_2)$	2573	2595	−22	A_1	4(98)	$\nu_s(CN)$	885	891	−6	A_1	2(45) + 7(38) − 6(12)
$\nu_a(ND_2)$	2563	2584	−21	B_2	15(99)	$\rho_a(ND_2)$	843	855	−12	B_2	18(76) − 13(15)
$\nu_s(ND_2)$	2423	2439	−16	A_1	3(97)	$\omega(CO)$	787	779	8	B_1	11(97)
$\nu_s(ND_2)$	2403	2431	−28	B_2	14(98)	$\tau_a(ND_2)$	533	550	−17	B_1	10(97)
$\nu(CO)$	1601	1603	−2	A_1	1(59) − 2(22) + 5(11)	$\delta(CO)$	527	508	19	B_2	16(74) + 18(24)
$\nu_a(CN)$	1506	1490	16	B_2	13(74) − 16(14)	$\delta(CN)$	459	466	−7	A_1	5(77) − 7(23)
$\delta_s(ND_2)$	1247	1251	−4	A_1	6(76) + 2(16)	$\tau_s(ND_2)$	428			A_2	8(100)
$\delta_a(ND_2)$	1147	1154	−7	B_2	17(89)	$\omega_a(ND_2)$	388	376	12	B_1	12(95)
$\rho_s(ND_2)$	991	1002	−11	A_1	7(37) − 1(24) − 2(19)	$\omega_s(ND_2)$	361			A_2	9(100)
					$C^{18}O(ND_2)_2$						
$\nu_a(ND_2)$	2573	2593	−20	A_1	4(98)	$\nu_s(CN)$	884	893	−9	A_1	2(46) + 7(37) − 6(12)
$\nu_a(ND_2)$	2563	2589	−26	B_2	15(99)	$\rho_a(ND_2)$	841	849	−8	B_2	18(77) − 13(14)
$\nu_s(ND_2)$	2423	2437	−14	A_1	3(97)	$\omega(CO)$	783	780	3	B_1	11(97)
$\nu_s(ND_2)$	2403	2431	−28	B_2	14(98)	$\tau_a(ND_2)$	531	560	−29	B_1	10(97)
$\nu(CO)$	1583	1590	−7	A_1	1(56) − 2(24) + 5(12)	$\delta(CO)$	514	507	7	B_2	16(75) + 18(23)
$\nu_a(CN)$	1505	1473	32	B_2	13(74) − 16(14)	$\delta(CN)$	456	461	−5	A_1	5(77) − 7(23)
$\delta_s(ND_2)$	1243	1276	−33	A_1	6(77) + 2(14)	$\tau_s(ND_2)$	428			A_2	8(100)
$\delta_a(ND_2)$	1147	1137	10	B_2	17(89)	$\omega_a(ND_2)$	388	378	10	B_1	12(96)
$\rho_s(ND_2)$	970	978	−8	A_1	7(38) − 1(28) − 2(18)	$\omega_s(ND_2)$	361			A_2	9(100)
					$CO(^{15}ND_2)_2$						
$\nu_a(ND_2)$	2556	2573	−17	A_1	4(98)	$\nu_s(CN)$	871	878	−7	A_1	2(47) + 7(39)
$\nu_a(ND_2)$	2547	2566	−19	B_2	15(99)	$\rho_a(ND_2)$	833	846	−13	B_2	18(77) − 13(15)
$\nu_s(ND_2)$	2415	2429	−14	A_1	3(98)	$\omega(CO)$	785	776	9	B_1	11(97)
$\nu_s(ND_2)$	2395	2422	−27	B_2	14(98)	$\tau_a(ND_2)$	532	550	−18	B_1	10(97)
$\nu(CO)$	1598	1600	−2	A_1	1(60) − 2(22) + 5(11)	$\delta(CO)$	524	512	12	B_2	16(74) + 18(23)
$\nu_a(CN)$	1492	1480	12	B_2	13(74) − 16(15)	$\delta(CN)$	455	463	−8	A_1	5(78) − 7(22)
$\delta_s(ND_2)$	1233	1239	−6	A_1	6(79) + 2(15)	$\tau_s(ND_2)$	428			A_2	8(100)
$\delta_a(ND_2)$	1144	1151	−7	B_2	17(90)	$\omega_a(ND_2)$	385	382	3	B_1	12(95)
$\rho_s(ND_2)$	983	993	−10	A_1	7(37) − 1(24) − 2(21)	$\omega_s(ND_2)$	357			A_2	9(99)

TABLE 8 (Continued)

assignment	ν_{calc}	ν_{exp}	δ^c	S^d	PED^e	assignment	ν_{calc}	ν_{exp}	δ^c	S^d	PED^e
					$^{13}CO(ND_2)_2$						
$\nu_a(ND_2)$	2573	2597	−24	A_1	4(98)	$\nu_s(CN)$	884	890	−6	A_1	2(45) + 7(38) − 6(12)
$\nu_a(ND_2)$	2563	2586	−23	B_2	15(99)	$\rho_a(ND_2)$	843	854	−11	B_2	18(76) − 13(15)
$\nu_s(ND_2)$	2423	2433	−10	A_1	3(98)	$\omega(CO)$	763	754	9	B_1	11(96)
$\nu_s(ND_2)$	2402	2430	−28	B_2	14(98)	$\tau_a(ND_2)$	533	559	−26	B_1	10(96)
$\nu(CO)$	1558	1576	−18	A_1	1(59) − 2(22) + 5(11)	$\delta(CO)$	526	505	21	B_2	16(74) + 18(24)
$\nu_a(CN)$	1469	1456	13	B_2	13(73) − 16(13)	$\delta(CN)$	457	473	−16	A_1	5(77) − 7(23)
$\delta_s(ND_2)$	1247	1249	−2	A_1	6(75) + 2(16)	$\tau_s(ND_2)$	428			A_2	8(100)
$\delta_a(ND_2)$	1142	1151	−9	B_2	17(87)	$\omega_a(ND_2)$	388	378	10	B_1	12(96)
$\rho_s(ND_2)$	990	1000	−10	A_1	7(37) − 1(23) − 2(20) + 5(10)	$\omega_s(ND_2)$	361			A_2	9(100)

[a] This study. [b] Parent molecule frequencies used in the least-squares determination of the optimal scale factors. [c] $\nu_{calc} - \nu_{exp}$. [d] Symmetry [e] Potential energy distribution. See Table 2 for the definition of the symmetry coordinates. The procentual contribution of each coordinate is given between parentheses. Only contributions larger than 10% are listed.

Vijay et al.,[17] however, assigned the two symmetric modes in reversed order. In addition they assigned the antisymmetric B_2 mode to a band at 3360 cm^{-1}, whereas most authors[4−6,10] assigned it to a band around 3440 cm^{-1}.

ν(CO) Mode and the Symmetric and Antisymmetric $\delta(NH_2)$ Modes. In the spectrum of the parent compound three bands are observed in the 1500−1700 cm^{-1} region. The band at 1627 cm^{-1} was assigned to the $\delta_a(NH_2)$ vibration. This is in accordance with most authors except Vijay et al.[17] and Saito et al..[57] The former assumed that the δ_a NH_2 vibration coincided with the $\delta_s(NH_2)$ vibration at 1545 cm^{-1}, whereas the latter assumed it coincided with the ν(CO) mode at 1615 cm^{-1}. Some authors[4−7] have assigned the band at 1683 cm^{-1} to the ν(CO) vibration and the band at 1598 cm^{-1} to the $\delta_s(NH_2)$ vibration, whereas others[8−11] assigned them in reversed order. From the calculated PED (see Table 8) it can be seen that according to our calculations the band at 1598 cm^{-1} is to be attributed to the C−O stretching vibration, although both bands contain contributions from both the C−O stretching vibration and the NH_2 deformation mode. This is in agreement with our experimental data.[12] The band at 1471 cm^{-1} was assigned to the antisymmetric C−N stretching vibration, in agreement with the data in the literature.

Symmetric and Antisymmetric $\rho(NH_2)$ Modes and the ν_s(CN) mode. The bands at 1149 and 1008 cm^{-1} have been assigned to the $\rho_s(NH_2)$ mode and the ν_s(CN) mode, respectively, in agreement with the data in the literature. The band at 1055 cm^{-1} was assigned to the $\rho_a(NH_2)$ mode. Some authors[5,8,57] assumed that this band coincides with the $\rho_s(NH_2)$ band, while Liapis et al.[6] assumed it to coincide with the ν_s(CN) mode.

ω(CO) Band and the Symmetric and Antisymmetric $\tau(NH_2)$ Bands. The band at 790 cm^{-1} is assigned to the ω(CO) vibration and the band at 727 cm^{-1} to the $\tau_a(NH_2)$ vibration. These assignments are in agreement with most authors except Vijay et al.[17] and Liapis et al.[6] The former assigned the $\tau_a(NH_2)$ vibration to a band at 565 cm^{-1} but did not assign the ω(CO) vibration, while the latter assigned the $\tau_a(NH_2)$ and the ω(CO) vibration to bands at 562 and 729 cm^{-1}, respectively. The $\tau_s(NH_2)$ mode is infrared inactive.

δ(CO), δ(CN), and the Symmetric and Antisymmetric $\omega(NH_2)$ Modes. Of these four modes only three are infrared active. The δ(CO) mode is observed at 568 cm^{-1}, the δ(CN) mode at 532 cm^{-1}, and the $\omega_a(NH_2)$ mode at 508 cm^{-1}. This is in agreement with most authors except Liapis et al.[6] who assigned these vibrations to bands at 560, 550, and 372 cm^{-1}, respectively. Vijay et al.[17] have assigned the δ(CO) mode to a band at 565 cm^{-1} and assumed that the δ(CN) and the $\omega_a(NH_2)$ mode coincide at 550 cm^{-1}. The $\omega_s(NH_2)$ is infrared inactive.

TABLE 9: Comparison of Experimental and Calculated Isotope Shifts (δ, cm^{-1}) in Going from the Parent to Deuterated Urea in the Gas Phase (δ = parent − deuterated, cm^{-1})

	δ_{calc}	δ_{exp}		δ_{calc}	δ_{exp}
$\nu_a(NH_2)$	919	900	$\rho_a(NH_2)$	188	
$\nu_a(NH_2)$	921	900	$\nu_s(CN)$	104	115
$\nu_s(NH_2)$	950	935	$\omega(CO)$	29	
$\nu_s(NH_2)$	951	935	$\delta(CO)$	55	61
$\nu(CO)$	24	11	$\omega_s(NH_2)$	108	
$\delta_a(NH_2)$	465		$\tau_a(NH_2)$	194	
$\delta_s(NH_2)$	370	371	$\delta(CN)$	76	
$\nu_a(CN)$	−21	−14	$\omega_a(NH_2)$	45	
$\rho_s(NH_2)$	181		$\tau_s(NH_2)$	100	

VI. Frequency Shifts

A. Isotopic Shifts. The calculated and experimental isotopic shifts are tabulated for the gas phase and the crystal phase, respectively, in Tables 9 and 10 and depicted in Figure 3. The root mean square deviation and the maximum difference are 14 and 21 cm^{-1} for the gas phase and 15 and 43 cm^{-1} for the crystal phase. The calculated isotopic shifts are in excellent agreement with experiment. The largest positive isotope shift (parent to deuterated compound in the gas phase: 951 cm^{-1} calculated; 935 cm^{-1} experimental), as well as the largest negative shifts (parent to deuterated compound in the crystal phase: −37 cm^{-1} calculated; −19 cm^{-1} experimental) are very well represented.

B. Gas-Phase to Crystal-Phase Shifts. Shifts in frequencies in going from the gas phase to the crystal phase are given in Table 11 and depicted in Figure 4. The root mean square deviation and maximum difference between theory and experiment are 14 and 31 cm^{-1}, respectively. From Figure 4 and in view of the fact that the experimental shifts in frequencies vary between −136 cm^{-1} and +98 cm^{-1}, agreement between theory and experiment can be termed as excellent. As can be seen (Table 11) for the parent compound, the ν(CO) decreases by approximately 135 cm^{-1} (−134 cm^{-1} calculated, −136 cm^{-1} experimental), while the ν(CN) increases by approximately 80 cm^{-1} (ν_a(CN), 83 cm^{-1} calculated, 77 cm^{-1} experimental; ν_s(CN), 79 cm^{-1} calculated, 48 cm^{-1} experimental). The shift in ν_s(CN), however, is overestimated by almost a factor of 2 for which we have no explanation at the moment. These shifts in ν(CO) and ν(CN) are in agreement with the calculated trends in geometry and force constants (shift in CO bond length, +0.04 Å; shift in CN bond length, −0.04 Å; shifts in ν(CO) force constant, −1.8 mdyne/Å; shifts in ν(CN) force constants, +1.1 mdyne/Å for ν_a(CN) and +1.6 mdyne/Å for ν_s(CN)). These facts can be attributed to hydrogen bonds present in the crystal phase which lengthen the CO bond and shorten the CN bond in an N−C═O structural unit in which the carbonyl oxygen is taking

TABLE 10: Comparison of Experimental and Calculated Isotopic Shifts (cm^{-1}) in Going from the Parent Compound to the Isotopomer Indicated for Urea in the Crystal Phase

	$C^{18}O(NH_2)_2$		$CO(^{15}NH_2)_2$		$^{13}CO(NH_2)_2$		$CO(ND_2)_2$		$C^{18}O(ND_2)_2$		$CO(^{15}ND_2)_2$		$^{13}CO(ND_2)_2$	
	δ_{calc}	δ_{exp}	δ_{calc}	δ_{exp}	δ_{calc}	δ_{exp}	δ_{calc}	δ_{exp}	δ_{calc}	δ_{exp}	δ_{calc}	δ_{exp}	δ_{calc}	δ_{exp}
$\nu_a(NH_2)$	0	1	12	11	0	−6	887	853	887	855	904	875	887	851
$\nu_a(NH_2)$	0	1	11	13	0	2	889	851	889	846	905	869	889	849
$\nu_s(NH_2)$	0	2	5	11	0	8	924	906	924	908	932	916	924	912
$\nu_s(NH_2)$	0	2	4	13	0	14	923	899	923	899	931	908	924	900
$\delta_s(NH_2)$	5	7	8	7	11	7	411	432	415	407	425	444	411	434
$\delta_a(NH_2)$	0	1	12	12	7	3	484	473	484	490	487	476	489	476
$\nu(CO)$	11	9	1	0	31	30	−4	−5	14	8	−1	−2	39	22
$\nu_a(CN)$	1	1	5	5	33	27	−37	−19	−36	−2	−23	−9	0	15
$\rho_s(NH_2)$	15	13	7	7	0	5	162	147	183	171	170	156	163	149
$\rho_a(NH_2)$	0	0	9	9	1	−1	219	200	221	206	229	209	219	201
$\nu_s(CN)$	11	3	21	21	0	−2	128	117	129	115	142	130	129	118
$\omega(CO)$	4	6	1	2	21	27	10	11	14	10	12	14	34	36
$\tau_a(NH_2)$	1	5	2	2	4	0	197	177	199	167	198	177	197	168
$\tau_s(NH_2)$	0		0		0		174		174		174		174	
$\delta(CO)$	13	7	6	6	2	5	49	60	62	61	52	56	50	63
$\delta(CN)$	5	4	7	1	2	1	82	66	84	71	85	69	83	59
$\omega_a(NH_2)$	0	3	3	8	0	−2	124	132	124	130	127	126	124	130
$\omega_s(NH_2)$	0		3		0		102		102		106		102	

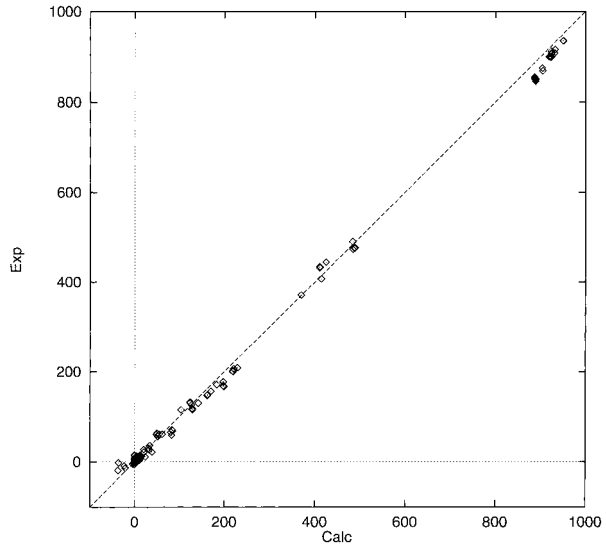

Figure 3. Plot of experimental (Exp) versus calculated (Calc) isotopic shifts (cm^{-1}) for urea in the crystal phase and the gas phase.

part in hydrogen bond formation, as explained above. While hydrogen bonding reduces the CO bond strength, it has the opposite effect on the out-of-plane movement of the OCN_2 unit. Calculations predict the frequency shifts to be only 12 cm^{-1}, but this is not verified experimentally.

Turning to the effect of hydrogen bonding upon frequencies related to N−H movements, it is expected that, similar to the effect on ν(CO), the $\nu(NH_2)$ frequencies should decrease. This is indeed verified experimentally as well as theoretically. Indeed ν(NH) stretching frequencies are found experimentally to decrease by between 95 and 113 cm^{-1} and calculated to decrease approximately 82−105 cm^{-1}.

While reducing stretch-related frequencies, hydrogen bonding should have the opposite effect upon valence angle deformation as well as out-of-plane movements involving hydrogen atoms. Again this is verified to high accuracy. The NH_2 out-of-plane mode is experimentally found to increase by 98 cm^{-1}, while the corresponding calculated increase is 90 cm^{-1}.

A similar trend is found for the valence angle movements $\rho_a(NH_2)$, $\delta_s(NH_2)$, and $\delta_a(NH_2)$ for which the increase in frequency is reproduced within 10−20%. Similar trends are found for the deuterated isotopomer.

TABLE 11: Comparison of Experimental and Calculated Shifts in Frequencies δ (δ = gas−crystal) (cm^{-1}) between the Gas Phase and the Crystal Phase of Urea

		$CO(NH_2)_2$		$CO(ND_2)_2$	
	S[a]	δ_{calc}	δ_{exp}	δ_{calc}	δ_{exp}
$\nu_a(NH_2)$	A_1	−82	−100	−50	−53
$\nu_a(NH_2)$	B_2	−90	−113	−57	−64
$\nu_s(NH_2)$	A_1	−88	−95	−62	−66
$\nu_s(NH_2)$	B_2	−105	−110	−77	−74
$\delta_s(NH_2)$	A_1	69	89	28	28
$\delta_a(NH_2)$	B_2	31	33	12	
$\nu(CO)$	A_1	−134	−136	−106	−120
$\nu_a(CN)$	B_2	83	77	99	82
$\rho_s(NH_2)$	A_1	4		23	
$\rho_a(NH_2)$	B_2	35	41	4	
$\nu_s(CN)$	A_1	79	48	55	46
$\omega(CO)$	B_1	12	0	31	
$\tau_a(NH_2)$	B_1	213		211	
$\tau_s(NH_2)$	A_2	256		181	
$\delta(CO)$	B_2	9	−10	15	−9
$\delta(CN)$	A_1	74		69	
$\omega_a(NH_2$	B_1	90	98	11	
$\omega_s(NH_2)$	A_2	−55		−49	

[a] Symmetry assignments are those based on a planar C_{2v} geometry.

The largest shifts in frequency in going from the gas phase to the crystal phase are predicted to be found for the $\tau(NH_2)$ modes (256 cm^{-1} for $\tau_s(NH_2)$, 213 cm^{-1} for $\tau_a(NH_2)$). However a very small intensity in infrared as well as in Raman spectra precludes experimental verification.

These calculated shifts are in agreement with the low-temperature and high-pressure spectroscopic measurements of the solid-state compound where we can consider the increasing amount of hydrogen bonding in the series gas-to-crystal phase to low-temperature crystal phase and gas-to-crystal phase to high-pressure crystal phase.[12]

VII. Conclusions

This study on urea in the gas phase and its $P\bar{4}2_1m$ crystal phase shows that accurate geometries, frequencies, and frequency shifts can be obtained by using the SM model even in the case of extensively hydrogen bonded systems such as urea. For the crystal phase, for which urea is modeled using a 15 molecule cluster surrounded by 5312 point charges, there is an excellent agreement between the calculated and experimental

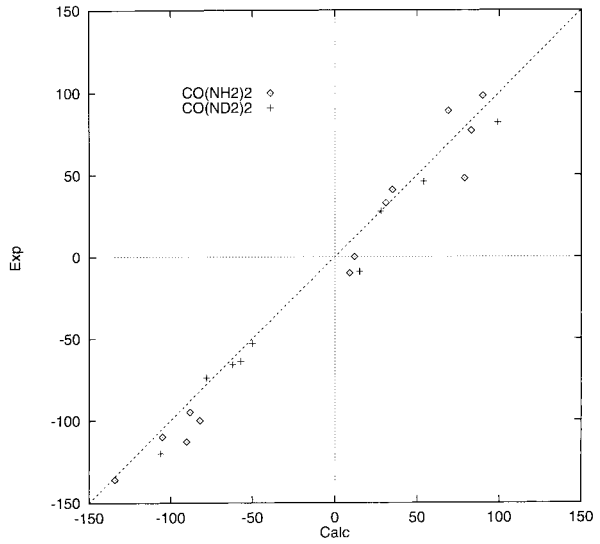

Figure 4. Plot of experimental (Exp) versus calculated (Calc) frequency shifts (cm^{-1}) for urea on going from the gas phase to the crystal phase.

geometries. For the gas phase there is a somewhat larger discrepancy between the calculated the experimental geometry, which is attributed to deficiencies in the procedure used to extract geometrical data from the observed rotational constants.

The excellent agreement between calculated and experimental frequencies for the $CO(NH_2)_2$, $C^{18}O(NH_2)_2$, $CO(^{15}NH_2)_2$, $^{13}CO(NH_2)_2$, $CO(ND_2)_2$, $C^{18}O(ND_2)_2$, $CO(^{15}ND_2)_2$ and $^{13}CO(ND_2)_2$ isotopomers of urea in the crystal phase and the $CO(NH_2)_2$, and $CO(ND_2)_2$ isotopomers of urea in the gas phase shows that the molecular cluster calculations yield accurate force fields and frequencies. Calculated isotopic shifts and gas-to-crystal phase shifts are in very good agreement with experiment, again indicating the applicability of the molecular cluster approach.

Acknowledgment. B.R. thanks the Flemish government institution IWT for a predoctoral grant. R.K. and C.V.A. thank the Flemish Science Foundation (FWO) for an appointment as "aspirant" and "onderzoeksdirecteur", respectively. H.O.D. thanks the FWO for financial support for the spectroscopic equipment. The authors gratefully acknowledge support by the University of Antwerp under Grant GOA-BOF-UA No. 23.

References and Notes

(1) Theophanides, T.; Harvey, P. D. *Coord. Chem. Rev.* **1987**, *76*, 237.
(2) Ledoux, I.; Zyss, J. *Chem. Phys.* **1982**, *73*, 203.
(3) Mathews, C. K.; Van Holde, K. E. *Biochemistry*, 2nd ed.; Benjamin/Cummings: Menlo Park, CA, 1996; p 4.
(4) Stewart, J. E. *J. Chem. Phys.* **1957**, *26*, 248.
(5) Hadzi, D.; Kidric, J.; Knezevic, Z. V.; Barlic, B. *Spectrochim. Acta A* **1976**, *32*, 693.
(6) Liapis, K.; Jayasooriya, U. A.; Kettle, S. F. A.; Eckert, J.; Goldstone, J. A.; Taylor, A. D. *J. Phys. Chem.* **1985**, *89*, 4560.
(7) Rajalakshmi, T.; Qhalid Fareed, R. S.; Dhanasekaran, R.; Ramasamy, P.; Thomas, J.; Srinivasan, K. *Mater. Sci. Eng. B* **1996**, *39*, 111.
(8) Yamaguchi, A.; Miyazawa, T.; Shimanouchi, T.; Mizushima, S. *Spectrochim. Acta* **1957**, *10*, 170.
(9) Laulicht, I.; Pinchas, S.; Petreanu, E.; Samuel, D. *Spectrochim. Acta* **1965**, *21*, 1487.
(10) Arenas, J.; Parellada, R. *J. Mol. Struct.* **1971**, *10*, 253.
(11) Duncan, J. L. *Spectrochim. Acta A* **1971**, *27*, 1197.
(12) Keuleers, R.; Rousseau, B.; Van Alsenoy, C.; Desseyn, H. O. To be published.
(13) Elbert, S. T.; Davidson, E. R. *Int. J. Quantum Chem.* **1974**, *8*, 857.
(14) Van Alsenoy, C.; Williams, J. O.; Schäfer, L. *J. Mol. Struct. (THEOCHEM)* **1981**, *76*, 179.
(15) Koizumi, M.; Tachibana, A.; Yamabe, T. *J. Mol. Struct. (THEOCHEM)* **1988**, *164*, 37.
(16) Williams, M. L.; Gready, J. E. *J. Comput. Chem.* **1989**, *10*, 35.
(17) Vijay, A.; Sathyanarayana, D. N. *J. Mol. Struct.* **1993**, *295*, 245.
(18) King, S. T. *Spetrochim. Acta A* **1972**, *28*, 165.
(19) Brown, R. D.; Godfrey, P. D.; Storey, J. *J. Mol. Spectrosc.* **1975**, *58*, 445.
(20) Li, X.; Stotesbury, S. J.; Jayasooriya, U. A. *Spectrochim. Acta A* **1987**, *43*, 1595.
(21) Godfrey, P. D.; Brown, R. D.; Hunter, A. N. *J. Mol. Struct.* **1997**, *413*−*414*, 405.
(22) Meier, R. J.; Coussens, B. *J. Mol. Struct. (THEOCHEM)* **1992**, *253*, 25.
(23) Ramondo, F.; Bencivenni, L.; Rossi, V.; Caminiti, R. *J. Mol. Struct. (THEOCHEM)* **1992**, *277*, 185.
(24) Kontoyianni, M.; Bowen, J. P. *J. Comput. Chem.* **1992**, *13*, 657.
(25) Gobbi, A.; Frenking, G. *J. Am. Chem. Soc.* **1993**, *115*, 2362.
(26) Ha, T.-K.; Puebla, C. *Chem. Phys.* **1994**, *181*, 47.
(27) Pisani, C.; Dovesi, R.; Roetti, C. *Hartree*−*Fock ab Initio Treatment of Crystalline Systems*; Lecture Notes in Chemistry, Vol. 48; Springer-Verlag: Berlin, 1988.
(28) Dovesi, R.; Causa', M.; Orlando, R.; Roetti, C.; Saunders: V. R. *J. Chem. Phys.* **1990**, *92*, 7402.
(29) Gatti, C.; Saunders: V. R.; Roetti, C. *J. Chem. Phys.* **1994**, *101*, 10686.
(30) Starikov, E. B. *Biopolymers* **1994**, *34*, 921.
(31) Saebø, S.; Klewe, B.; Samdal, S. *Chem. Phys. Lett.* **1983**, *97*, 499.
(32) Ángyán, J. G.; Silvi, B. *J. Chem. Phys.* **1987**, *86*, 6957. Bridet, J.; Fliszár, S.; Odiot, S.; Pick, R. *Int. J. Quantum Chem.* **1983**, *24*, 687. Sugano, S.; Shulman, R. G. *Phys. Rev.* **1963**, *130*, 517.
(33) Popelier, P.; Lenstra, A. T. H.; Van Alsenoy, C.; Geise, H. J. *J. Am. Chem. Soc.* **1989**, *111*, 5658. Lenstra, A. T. H.; Van Alsenoy, C.; Verhulst, K.; Geise, H. J. *Acta Crystallogr. B* **1994**, *50*, 96.
(34) Peeters, A.; Van Alsenoy, C.; Lenstra, A. T. H.; Geise, H. J. *Int. J. Quantum Chem.* **1993**, *46*, 73. Peeters, A.; Van Alsenoy, C.; Lenstra, A. T. H.; Geise, H. J. *J. Mol. Struct. (THEOCHEM)* **1994**, *304*, 101. Peeters, A.; Van Alsenoy, C.; Lenstra, A. T. H.; Geise, H. J. *J. Chem. Phys.* **1995**, *103*, 6608.
(35) Van Alsenoy, C. *J. Comput. Chem.* **1988**, *9*, 620.
(36) Van Alsenoy, C.; Peeters, A. *J. Mol. Struct. (THEOCHEM)* **1993**, *286*, 19.
(37) Almlöf, J.; Faegri, K.; Korsell, K. *J. Comput. Chem.* **1982**, *3*, 385.
(38) Van Alsenoy, C.; Rousseau, B. Manuscript in preparation.
(39) Van Alsenoy, C.; Yu, C.-H.; Peeters, A.; Martin, J. M. L.; Schäfer, L. *J. Phys. Chem.*, submitted for publication.
(40) Swaminathan, S.; Craven, B. M.; McMullan, R. K. *Acta Crystallogr. B* **1984**, *40*, 300.
(41) Mulliken, R. S. *J. Chem. Phys.* **1955**, *23*, 1833.
(42) Pulay, P. *Mol. Phys.* **1969**, *17*, 197. Pulay, P. *Theor. Chim. Acta* **1979**, *50*, 299. Pulay, P. In *Ab initio methods in quantum chemistry*, Part II; Advances in Chemical Physics, Vol. LXIX; Lawley, K. P., Ed.; Wiley: New York, 1987; p 241.
(43) Wilson, E. B., Jr.; Decius, J. C.; Cross, P. C. *Molecular Vibrations*; McGraw-Hill: New York, 1955.
(44) Korn, E. D. In *Methods in Enzymology*, Vol. IV; Colowick, S., Kaplan N. O., Eds.; Academic Press: New York, 1957; p 623.
(45) Slootmaekers, B.; Desseyn, H. O. *Appl. Spectrosc.* **1991**, *45*, 118.
(46) Keller, W. E. *J. Chem. Phys.* **1948**, *16*, 1003.
(47) Waldron, R. D.; Badger, R. M. *J. Chem. Phys.* **1950**, *18*, 566.
(48) Andrew, E. R.; Hyndman, D. *Proc. Phys. Soc. A* **1953**, *66*, 1187. Andrew, E. R.; Hyndman, D. *Discuss. Faraday Soc.* **1955**, *19*, 195.
(49) Worsham, J. E., Jr.; Levy, H. A.; Peterson, S. W. *Acta Crystallogr.* **1957**, *10*, 319.
(50) Kraitchman, J. *Am. J. Phys.* **1953**, *21*, 17.
(51) Schwendeman, R. H. *Critical Evaluation of Chemical and Structural Information*; National Academy of Sciences: Washington, D.C., 1974; p 94. Costain, C. C. *Trans. Am. Cryst. Soc.* **1966**, *2*, 157.
(52) Popelier, P.; Lenstra, A. T. H.; Van Alsenoy, C.; Geise, H. J. *Struct. Chem.* **1991**, *2*, 3.
(53) Allen, F. H.; Bellard, S.; Brice, M. D.; Cartwright, B. A.; Doubleday, A.; Higgs, H.; Hummelink, T.; Hummelink-Peters, B. G.; Kennard, O.; Motherwell, W. D. S.; Rodgers, J. R.; Watson, D. G. *Acta Crystallogr. B* **1979**, *35*, 2331.
(54) Pulay, P.; Fogarasi, G.; Boggs, J. E. *J. Chem. Phys.* **1981**, *74*, 3999. Fogarasi, G.; Pulay, P. Ab Initio Calculation of Force Fields and Vibrational Spectra. In *Vibrational Spectra and Structure*; Durig, J. R., Ed.; Elsevier Science: Amsterdam, 1985.
(55) Langer, J.; Schrader, B.; Bastian, V.; Jacob, E. *Fresenius J. Anal. Chem.* **1995**, *352*, 489.
(56) Spoliti, M.; Pieretti, A.; Bencivenni, L.; Sanna, N. *Electron. J. Theor. Chem.* **1997**, *2*, 149.
(57) Saito, Y.; Machida, K.; Uno, T. *Spectrochim. Acta A* **1971**, *27*, 991.